BIODIVERSITAS
Volume 26, Number 1, January 2025
Pages: 296-305

ISSN: 1412-033X
E-ISSN: 2085-4722
DOI: 10.13057/biodiv/d260129

Teliospore morphology characterization of *Uromycladium falcatariae* in falcata plantations at different elevations in Mindanao Island, Philippines

MHAR O. LOQUEZ[1,2,♥], CAROLINA D. AMPER[2], ADRIAN M. TULOD[3,4], DENNIS M. GILBERO[5]

[1]Forest and Wetland Research Development and Extension Center, Ecosystems Research and Development Bureau. Maharlika, Bislig City 8311, Surigao del Sur, Philippines. Tel.: +63-495362269, ♥email: mharloquez@gmail.com

[2]Department of Plant Pathology, College of Agriculture, Central Mindanao University. Musuan 8714, Bukidnon, Philippines

[3]Institute of Renewable Natural Resources, College of Forestry and Natural Resources, University of the Philippines Los Baños. Pedro R. Sandoval Ave, Los Baños 4031, Laguna, Philippines

[4]Department of Forest Biological Sciences, College of Forestry and Environmental Science, Central Mindanao University. Musuan 8714, Bukidnon, Philippines

[5]Sustainable Agro-Biomaterials Research Laboratory, College of Agriculture, Agusan del Sur State College of Agriculture and Technology. Bunawan 8506, Agusan del Sur, Philippines

Manuscript received: 4 August 2024. Revision accepted: 18 January 2025.

Abstract. *Loquez MO, Amper CD, Tulod AM, Gilbero DM. 2025. Teliospore morphology characterization of* Uromycladium falcatariae *in falcata plantations at different elevations in Mindanao Island, Philippines. Biodiversitas 26: 296-305.* The fungus *Uromycladium falcatariae* causes gall rust disease in falcata (*Falcataria falcata*), with severe infections commonly observed at higher elevations (>400 masl). It produces teliospores that disperse through the air, contributing to its widespread prevalence. This study aimed to characterize the fungal teliospores across different elevations in Mindanao using Light Microscopy (LM) and Scanning Electron Microscopy (SEM). Mature galls with visible brown or rusty powder from falcata were collected from low (<400 masl), moderate (>400-800 masl), and high (>801 masl) elevations. Microphotographs of the teliospores were generated, examined, and compared for morpho-features and quantitative measurements across these elevations. This research provides the first SEM-based morphological characterization of *U. falcatariae*. The LM results revealed significant increases in teliospore length ($P<0.05$) and width ($P<0.05$) with elevation, with the largest dimensions observed at high elevations. SEM analysis demonstrated significant variation in the diameter of the germ pore ($P<0.01$) and the dorsal concave structure ($P<0.05$) across elevations, with the largest measurements recorded at high elevations. Detailed morphological features and quantitative measurements of teliospores were revealed from apical, dorsal, and equatorial orientations in SEM. Furthermore, this study provided morphological characteristics of teliospores across elevations, which can aid in the taxonomy and morphological classification of this rust fungus.

Keywords: Elevation, gall rust, falcata, Mindanao Island, morphology, *Uromycladium falcatariae*, teliospore

INTRODUCTION

Falcata (*Falcataria falcata* (L.) Greuter & R. Rankin) is a multipurpose tree species native to Indonesia, Papua New Guinea, and the Solomon Islands. It is extensively cultivated across Asia, particularly in the Philippines (Krisnawati et al. 2011; Rojas-Sandoval 2023). On Mindanao Island, falcata is one of the most prevalent exotic species, typically planted in monoculture or intercropping systems (Santos et al. 2010). This species contributes approximately 71.64%, or 592,485 m³, of the Philippines' total log production (FMB-DENR 2021). Its uses range from pulp and lightweight packaging materials to paper, veneer plywood, furniture, and light construction materials. Additionally, it is valued for its soil conservation potential due to nitrogen fixation (Doloriel 2017; Alipon et al. 2021; Marasigan et al. 2022). Its fast growth and short rotation cycle make it highly favored for plantations and agroforestry applications even at higher elevations for production.

Despite its economic and ecological significance, falcata plantations face severe challenges from pests and diseases in the region (Rahayu et al. 2021; Rojas-Sandoval 2023; Tulod et al. 2024). Among these, gall rust caused by *Uromycladium falcatariae* Doungsa-ard, McTaggart, Geering & R.G. Shivas is a particularly destructive disease affecting plantations across Southeast Asia. This microcyclic fungus, which produces wind-dispersed teliospores that remain viable for several months and complete its life cycle on a single host, falcata (Wood 2022). The pathogen enters through direct penetration, natural opening, or wound-forming chocolate brown, cauliflower- or whip-like galls on stems, branches, leaf petioles, and shoots, inflicting substantial damage at all growth stages and affecting its growth and yield performance (Rahayu et al. 2009; Rahayu et al. 2010; Rahayu et al. 2018, Rahmawati et al. 2019). Incidence of the disease correlates with elevation, with minimal infection at low elevations and increasing severity at higher altitudes, which promotes disease development with high relative humidity and low wind speed (Lacandula et al. 2017; Rahayu et al. 2018). Addressing this disease requires comprehensive understanding of both environmental factors and the pathogen's morphological characteristics to inform effective management strategies.

Earlier studies identified the fungus as *Uromycladium tepperianum* (Sacc.) McAlpine is based on striation patterns observed in teliospores which is also used to differentiate

other *Uromycladium* species (Eusebio 1998; Rahayu et al. 2010; Doungsa-ard et al. 2015). While *U. tepperianum* is known to cause severe gall rust infections in *Acacia* species, including falcata, Doungsa-ard et al. (2015) described *U. falcatariae* as a distinct taxon based on molecular sequences, teliospore wall morphology, and its host genus of the Memosoideae tribe Ingeae (*Falcataria*) and Acacieae (*Acacia*). The species is characterized by unique morphological features, including 25-32 striae on the teliospore wall. Subsequent research by Lelana et al. (2022) in Indonesia revealed distinct genetic characteristics and variations in teliospore dimensions and striae counts, ranging from 25 to 38, that may have evolved and adapted to its host population. Several factors including host specificity, environmental conditions, genetic diversity, geographical isolation, and even human activities influence the variability of the pathogen's morpho-structure and genetic components. Likewise, obligate parasites like rust fungus are known to infect plants where they interact and co-evolve (Chowdhury et al. 2022). Hence, requires comprehensive studies of the pathogen's evolutionary characteristics with its complex nature.

Morphological and molecular approaches play a pivotal role in understanding the pathogen's characteristics including its interaction with the host plant and survival in the environment. Although light microscopy has provided initial insights into the morphological characteristics of *U. falcatariae* (Doungsa-Ard et al. 2015; Lelana et al. 2022), detailed characterization using high-resolution techniques like Scanning Electron Microscopy (SEM) remains limited. SEM offers the ability to reveal comprehensive details of teliospore structures, facilitating pathogen variability assessment and taxonomic classification (Ijaz et al. 2022). It is hypothesized that the morphological characteristics of *U. falcatariae* teliospores vary with elevation. Thus, this investigation aimed to characterize the morphological features and quantitative measurements of teliospores from rust fungus across different elevations in Mindanao, Philippines, using both light microscopy and SEM.

MATERIALS AND METHODS

Study area

The study was conducted in selected falcata plantations across varying elevations on Mindanao Island, Philippines, a region where the species is extensively cultivated, particularly in the Caraga Region (R13), known as the timber corridor, and Northern Mindanao (R10). Two plantations were identified and categorized into three elevation levels: low (0-400 m asl), moderate (400-800 masl), and high (>800 masl). These classifications were based on previous reports regarding the occurrence and severity of gall rust disease in falcata, with slight modifications to the elevation ranges. Basic plantation data, including GPS coordinates, were collected to map the distribution of the plantations (Table 1 and Figure 1).

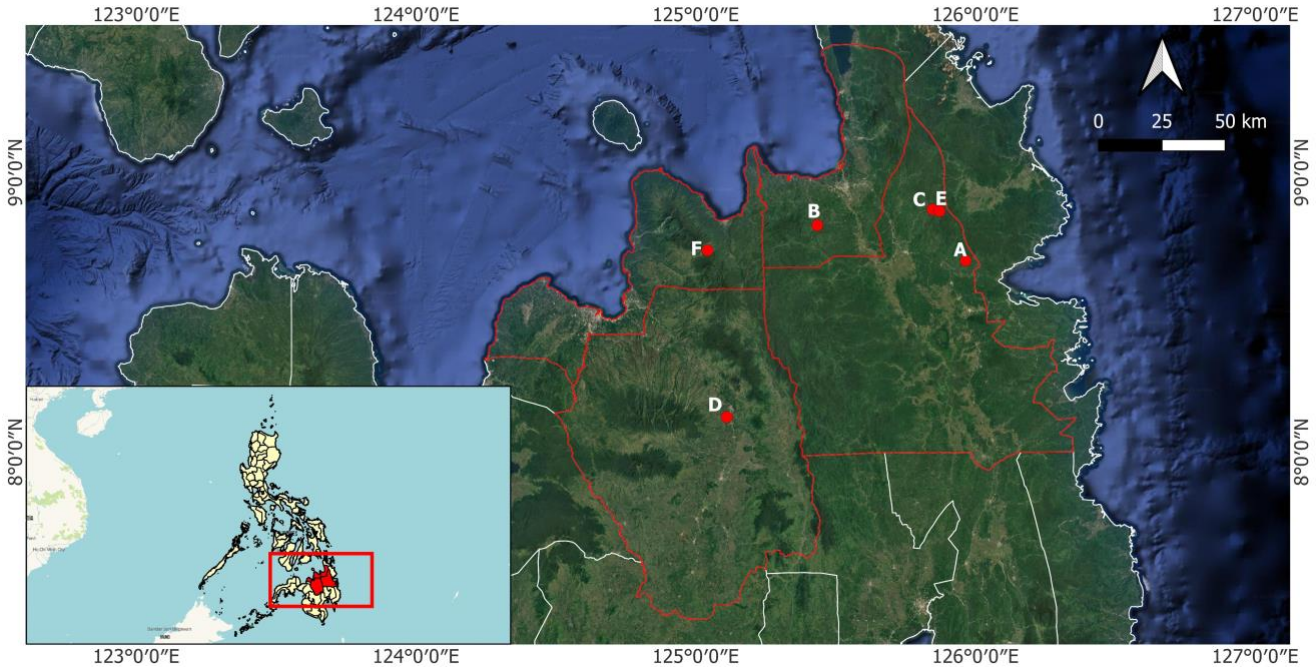

Figure 1. Map of the sampling sites at different elevation levels of falcata plantations in Mindanao. Low: A (157 masl); B (274 masl), Moderate: C (659 masl); D (698 masl), High: E (696 m asl.); F (1029 m asl.)

Table 1. Sampling site description of the falcata plantation of the study

Elevation level	Falcata stand	Elevation (masl)	Age (yrs)	Slope	Location	GPS coordinates
Low	A	157	2	Rolling	Mabuhay, Prosperidad, Agusan del Sur	8°41' 6" N, 125°57'55" E
	B	274	7	Rolling	Simbalan, Buenavista, Agusan del Norte	8°48'40" N, 125°26' 6" E
Moderate	C	659	8	Rolling	San Juan, Bayugan City, Agusan del Sur	8°52'4" N, 125°50'48" E
	D	698	4	Undulating	Sta. Ana, Malaybalay City, Bukidnon	8°7'30" N, 125°6'41" E
High	E	969	8	Rolling	San Juan, Bayugan City, Agusan del Sur	8°51' 41"N, 125°52'19" E
	F	1029	3	Rolling	Lunotan, Gingoog City, Misamis Oriental	8°43'17" N, 125°2'32" E

Sample collection

Mature galls observed on twigs and leaf petioles of falcata, characterized by visible brown/rusty teliospores on their surface (Figures 2C-2.D), were collected from the identified sampling sites. Each gall was placed in plastic containers, stored in an ice box, and transported to the Pest and Disease Laboratory of the Forest and Wetland Research Development and Extension Center (FWRDEC) in Bislig City, Surigao del Sur, Philippines. The typical structure of gall rust disease observed in the plantation was meticulously documented, with a particular focus on infection sites on falcata trees, ensuring the highest level of accuracy.

Morphological characterization

Light Microscopy (LM)

The teliospores were carefully mounted on glass slides with clear glycerin and examined under a T720-AM scope trinocular compound microscope at 400× magnification. Microphotographs of the fungal teliospores were captured using the S-EYE 1.10.7 application on the microscope's built-in tablet and camera, facilitating their characterization and comparison.

Scanning Electron Microscopy (SEM)

The teliospores were aseptically extracted from the gall surface using a soft brush, carefully placed in a test tube with a cover, and stored in a refrigerator. The samples were submitted to the Department of Chemistry at Ateneo de Davao University, Davao City, for SEM analysis. They were coated with a gold/palladium alloy for 1 minute at 10 mA and examined using the Hitachi SU1510 SEM instrument at 1,000×, 5,000×, and 7,000× magnifications, generating micrographs of the fungal teliospores.

The generated micrographs from LM and SEM were measured using the ImageJ application. A total of 150 teliospores from LM were analyzed based on their dimensions, color, shape, and wall thickness. In the SEM analysis, 20 teliospores from the generated micrographs were examined for morpho-features, such as surface structure and ornamentation, as well as quantitative measurements, including equatorial width, number of striae, distance between equatorial striae, germ pore diameter, and dorsal concave diameter.

The characterization was based on existing data on the rust fungus (Rahayu et al. 2010; Doungsa-ard et al. 2015; Wood 2019; Lelana et al. 2022) and other LM and SEM studies of related organisms (Khan et al. 2020; Han et al. 2021; Ijaz et al. 2022).

Data analysis

The numeric data were summarized descriptively, including the minimum, maximum (in parentheses), and average ± standard deviation. Analysis of variance (ANOVA) was performed on the teliospore quantitative measurements using IBM SPSS version 24 (IBM Corp 2016) to determine differences across elevation ranges. Additionally, Tukey's HSD test was applied for post-hoc analysis. A comparative analysis was conducted on the morphological features and quantitative measurements obtained from the LM and SEM micrographs of the fungal teliospores.

RESULTS AND DISCUSSION

Gall rust symptoms in the falcata plantation caused by *U. falcatariae* were observed on the trunk (Figure 2.A), branches (Figure 2.B), leaf petioles (Figure 2.C), leaf rachis (Figure 2.D), and pods (Figure 2E). The disease produces a reddish-brown or rusty powder on the surface of the galls, known as teliospores. The current study presents the morphological characteristics of the teliospores observed through LM and SEM (Table 2). Likewise, the morpho-characteristics of the *U. falcatariae* from the previous studies using light microscopy (Table 5).

Table 2. Morphological comparison of the teliospores in LM and SEM micrograph of *Uromycladium falcatariae*

Morphological features	Light Microscopy (LM)	Scanning Electron Microscopy (SEM)
Shape	Globose to sub-globose	Apical and Dorsal View: Globose to sub-globose Equatorial View: Oblate/ ellipsoid/ reniform
Teliospore structure	Solitary germ pores (apical) and depressed structure (dorsal), Thick-walled and striated at the edge	Germ pore (Apical), Concaved (Dorsal), Longitudinal striation (Equatorial)
Color	Yellowish brown, reddish brown to brown	
Surface ornamentation	-	A few small and large warts (verrucose) and some covers/overlaps on the germ pore, striae, and dorsal concave -Dense at high elevation

A comparative analysis of the morphological micrographic features under light microscopy is shown in Figure 3, while the SEM images are presented in Figures 4, 5, and 6. The quantitative morpho-characteristics of the teliospores across different elevation ranges observed under LM are summarized in Table 3, and those under SEM are presented in Table 4.

Morphological micrographic features

In light microscopy, the teliospore characteristics of the fungus exhibited a globose/sub-globose shape, with colors varying from yellowish-brown to reddish-brown or brown. Three clustered teliospores were observed (Figure 3.G). The teliospore structure displayed thick walls, with visible striations around the edges (Figure 3.H), a solitary germ pore at the apex (Figure 3.I), and a dorsally depressed structure at the base (Figure 3.J).

Table 3. Quantitative morpho-characteristics of the teliospore *of Uromycladium falcatariae* using light microscopy across elevation levels of falcata plantation

Elevation level	Falcata stand	Teliospore length (µm)		Teliospore width (µm)		Wall thickness (µm)	
		Min-max	Ave	Min-max	Ave	Min-Max	Ave
Low	A	16.08-23.52	19.33±1.40^{c}	14.46-20.90	17.76±1.28^{b}	1.35-2.45	1.92±0.21
	B	16.94-24.62	19.88±1.16^{bc}	16.08-23.52	18.35±1.40^{ab}	1.24-2.45	1.76±0.23
Moderate	C	17.90-25.67	21.28±1.69^{ab}	13.62-23.42	18.63±1.51^{ab}	1.23-2.38	1.80±0.24
	D	15.90-24.24	20.74±1.45^{abc}	14.53-22.09	18.08±1.45^{ab}	1.22-2.29	1.72±0.24
High	E	17.76-25.19	21.34±1.55^{ab}	13.67-23.18	18.49±1.26^{ab}	1.25-2.31	1.73±0.25
	F	17.19-26.26	21.84±1.71^{a}	13.87-23.10	19.15±1.61^{a}	1.29-2.67	1.79±0.25
F-test			*		*		ns
%CV			5.01		3.15		5.27

Notes: Means with the same letter in a column are not significantly different at a 5% level of probability based on Tukey's HSD test. *significant, Ns: non-significant

Figure 2. Typical gall rust symptoms (A-D) with matured brown/rusty powder/teliospores (B-D) of *Uromycladium falcatariae* observed on it's A. Falcata stem; B. Branch; C. Leaf petiole; D. Leaf rachis; and E. Pods

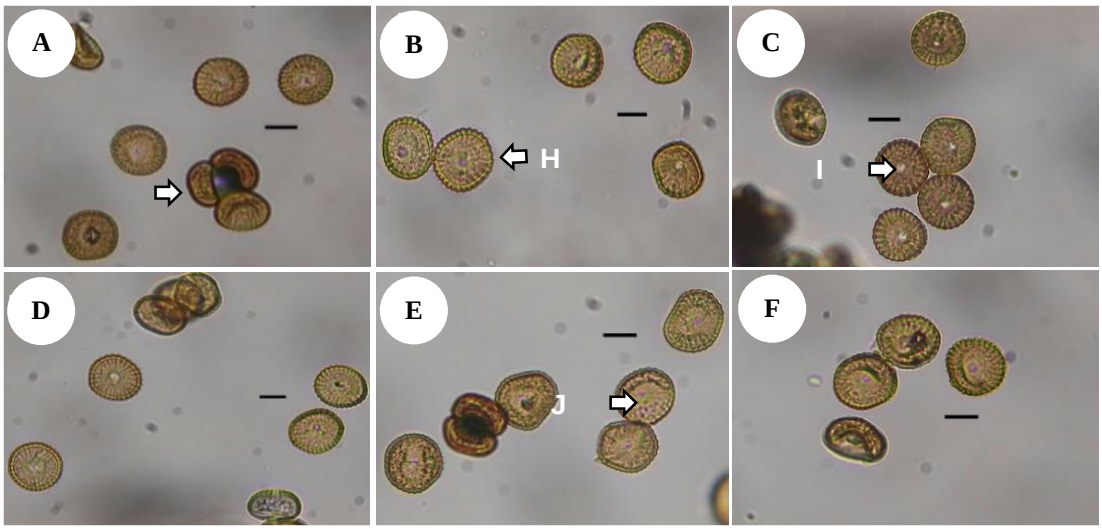

Figure 3. Teliospores of *Uromycladium falcatariae* under light microscopy at A-B. Low; C-D. Moderate; E-F. High elevation level-400×. G: 3 clustered teliospores, H: Distinct spore wall and striated edge, I: Germ pore, J: Dorsally depressed structure. (Scale bar 10 µm)

Table 4. Quantitative morpho-characteristics of the teliospore of *Uromycladium falcatariae* using scanning electron microscopy (SEM) across elevation levels of falcata plantation

Elevation level	Falcata stand	No. of striae		Equatorial width (µm)		Distance between equatorial striae (µm)		Germ pore (µm)		Dorsal concave (µm)	
		Min-Max	Ave	Min-Max	Ave	Min-Max	Ave	Min-Max	Ave	Min-Max	Ave
Low	A	28-37	31.60±2.66	6.30-12.85	7.88±1.65	0.70-2.38	1.63±0.30	0.44-2.23	1.19±0.61b	6.77-10.90	8.75±1.05a
	B	25-40	31.55±4.14	5.47-13.40	8.34±2.16	0.78-2.78	1.54±0.31	0.81-2.65	1.67±1.61a	5.30-11.95	8.71±1.54a
Moderate	C	26-37	31.20±2.88	5.57-9.23	7.27±1.08	0.88-2.47	1.68±0.18	0.69-1.85	1.18±0.31b	5.42-10.78	7.51±1.36b
	D	27-37	30.35±2.81	5.44-13.47	7.85±1.90	0.92-2.53	1.52±0.23	0.70-2.12	1.20±0.40b	5.33-11.61	8.84±1.54a
High	E	25-37	31.45±3.44	5.93-9.24	7.26±1.05	0.64-2.44	1.53±0.29	0.84-2.66	1.73±0.58a	7.04-11.86	9.42±1.18a
	F	25-35	30.05±2.67	4.39-14.48	8.08±2.63	0.67-2.63	1.69±0.33	1.08-2.46	1.80±0.40a	6.56-12.53	8.84±1.85a
F-test			ns		ns		ns		**		*
%CV			10.11		23.60		17.20		36.62		17.56

Notes: Means with the same letter in a column are not significantly different at a 5% level of probability based on Tukey's HSD test. **: highly significant, *: significant, ns-non-significant

Table 5. Morpho-characteristics of the *Uromycladium falcatariae* from the previous studies using light microscopy

Country	Dimension (µm)	Ave	No. of striations	Germ pore diameter (µm)	Color	Shape	References
Philippines	17.7-26.0 × 19.8-25.2	21.8 × 21.9			Yellowish brown	Globose	Eusebio (1998)
Philippines/Timor Leste	17-24 × 13-21	15-19 × 18-22	25-32	2.5-4 um	Yellowish brown	Globose or sub-globose	Doungsa-Ard et al. (2015)
Malaysia	17-26 × 13-18						Rahayu et al. (2010)
Indonesia	17-28 × 14-20						
West Java, Indonesia	18-26 × 16-24	21.35 × 19.75	27-35		Brown	Globose or sub-globose	Lelana et al. (2022)
Central Java, Indonesia	19-24 × 17-22	21.85 × 20.15	25-38				
East Java, Indonesia	18-25 × 18-23	21.35 × 19.45	26-34				
Beng, Indonesia	20-24 × 18-22	22.74 × 20.08	28-37				

In scanning electron microscopy, teliospores appeared as globose/sub-globose in both the apical and dorsal views and oblate/ellipsoid/reniform in the equatorial view. The teliospore orientation from apical, basal, and equatorial views revealed the primary surface ornamentation of the fungus. In the apical view, a solitary germ pore at the apex, with both open and closed structures, was observed across elevations (Figures 6.A-6.F). Additionally, the area surrounding the germ pore displayed various ornamentation patterns, including reticulate (Figures 6.C-6.D), rugulate (Figure 6.A), striated (Figures 6.B-6.C), and striated/ verrucose (Figure 6.F). The base of the teliospore exhibited a dorsal concave structure (Figures 5.A-5.F), and the equatorial view revealed visible striations. Furthermore, streaks on the teliospores started from the dorsal concave edge (Figures 5.A-5.F) and converged longitudinally towards the germ pore (Figures 6.A-6.F).

The morphological features of the teliospores observed in LM and SEM were consistent across different elevations. However, SEM revealed surface ornamentation, which varied from small to large verrucose coverings or overlapping striae (Figures 6.B-6.E), the germ pore (Figures 5.A-5.B), and the dorsal concave (Figures 5.A-5.F). These features were particularly dense at higher elevations (Figure 4.F).

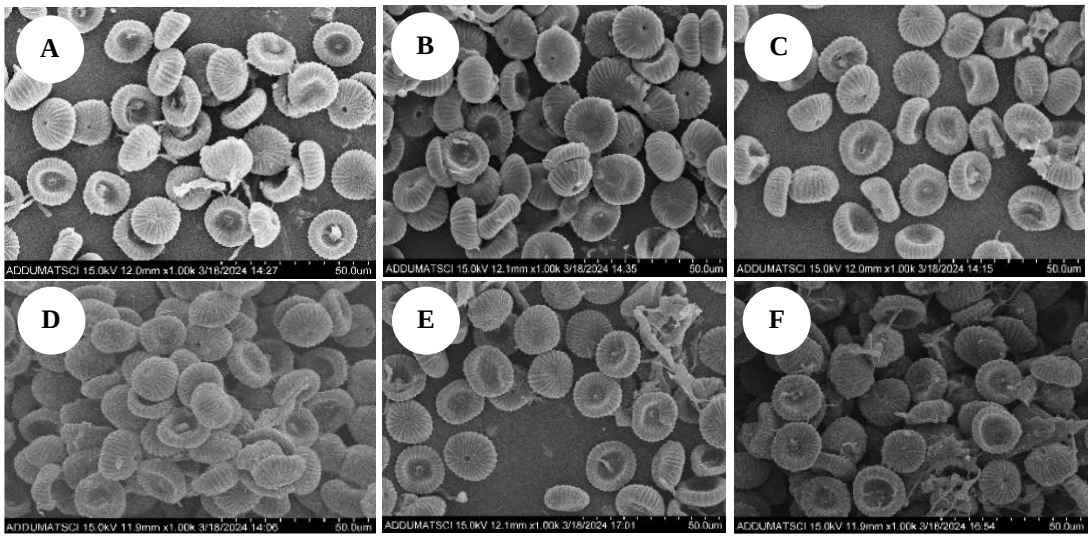

Figure 4. Scanning electron microphotographs of the teliospores of *Uromycladium falcatariae* at A-B. Low; C-D. Moderate; E-F. High elevation levels

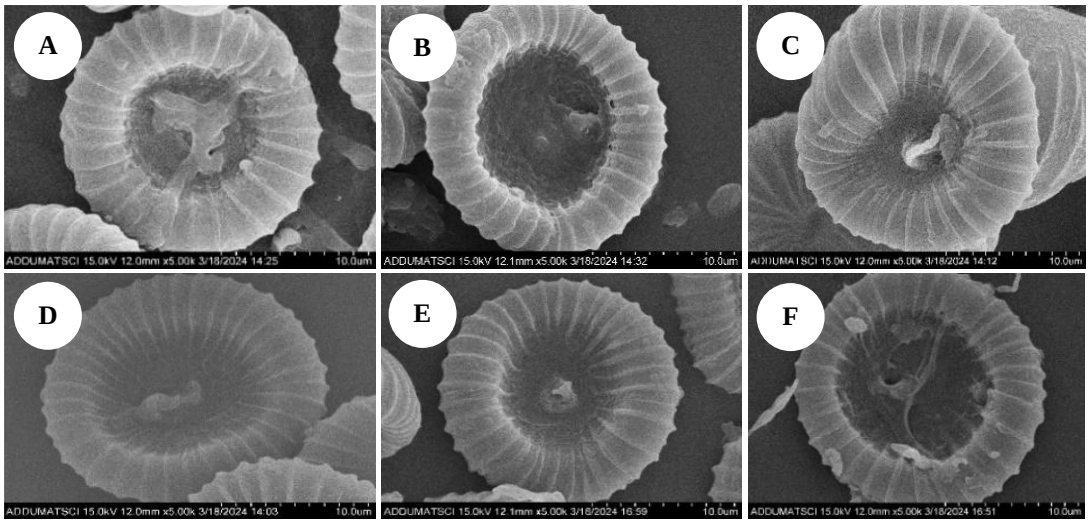

Figure 5. The dorsal concave of the teliospores under scanning electron microscopy of *Uromycladium falcatariae* at A-B. Low; C-D. Moderate; E-F. High elevation levels

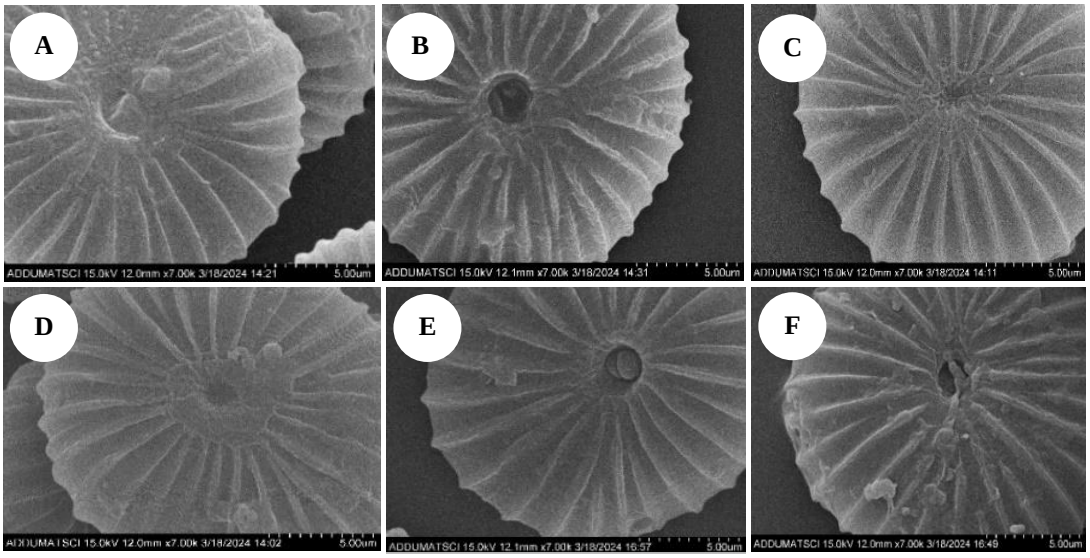

Figure 6. Apical germ pore of the teliospores under scanning electron microscopy of *Uromycladium falcatariae* at A-B. Low; C-D. Moderate; E-F. High elevation levels

Morphological quantitative measurements

Results from LM analysis revealed significant variation in teliospore length and width, which could potentially impact the reproductive success and survival of falcata. In contrast, no significant difference was observed in wall thickness at different elevations of falcata plantations in Mindanao (Table 3). The teliospore length varied from 15.90 to 26.26 µm, with the minimum range spanning from 15.90-17.76 µm, and the maximum range from 23.52-26.26 µm. The longest teliospore length was recorded at high elevation (F) with 21.84 µm, which was comparable to high elevation (E) and moderate elevation (C and D) with lengths of 21.34 µm, 21.28 µm, and 20.74 µm, respectively. However, it differed significantly from the shortest lengths recorded at low elevation (B) and (A) with 19.88 µm and 19.33 µm, respectively. The teliospore width varied from 13.67 to 23.52 µm, with the minimum range spanning 13.67-16.08 µm and the maximum range from 20.90-23.52 µm. The widest teliospore was observed at high elevation (F) with 19.15 µm, which was not comparable to low elevation (A) with 17.76 µm. Furthermore, the wall thickness of the teliospore ranged from 1.22 to 2.67 µm, with the minimum range from 1.22-1.33 µm and the maximum range from 2.29-2.67 µm. The thickest wall was recorded at low elevation (A) with 1.92 µm, while the thinnest was observed at moderate elevation (D) with 1.72 µm.

SEM analysis revealed highly significant variation in germ pore diameter and significant variation in dorsal concave diameter, while no significant variation was observed in the number of striae, equatorial width, and distance between equatorial striae at different elevations of falcata plantations in Mindanao (Table 4). The germ pore diameter varied from 1.19 to 3.66 µm, with the minimum range from 0.44-1.08 µm and the maximum range from 1.85-2.66 µm. The largest germ pore diameter was recorded at high elevation (F), followed by (E) and low elevation (B), with values of 1.80 µm, 1.73 µm, and 1.67 µm, respectively. These were not comparable to moderate elevations (C and D) and low elevation (A), where diameters of 1.18 µm, 1.20 µm, and 1.19 µm were recorded, respectively, representing the smallest diameters. The dorsal concave diameter ranged from 5.30 to 12.53 µm, with the minimum range from 5.30-7.04 µm and the maximum range from 10.78-12.53 µm. The largest dorsal concave diameter was observed at high elevation (E) with 9.42 µm, followed by high elevation (F) and moderate elevation (D) with averages of 8.84 µm, and low elevation (A and B) with 8.75 µm and 8.71 µm, respectively.

However, this differed significantly from moderate elevation (C), which recorded the smallest diameter at 7.51 µm. The number of striae ranged from 25 to 40 striae, with the minimum range from 25-28 striae and the maximum range from 35-40 striae. The highest number of striae was recorded at low elevation (A) with 31.55, while the lowest was observed at moderate elevation with 30.35. The equatorial teliospore width at different elevations ranged from 4.39 to 14.48 µm, with the minimum range from 4.39-6.30 µm and the maximum range from 9.23-14.48 µm, observed primarily at site (F). The widest teliospore was observed at low elevation (B) with 8.34 µm, while the narrowest was at high elevation (E) with 7.26 µm. The distance between equatorial striae ranged from 0.64 to 2.78 µm, with the minimum range from 0.64-0.92 µm and the maximum range from 2.38-2.78 µm. The longest distance was recorded at high elevation (F) with 1.69 µm, while the shortest was at moderate elevation (D) with 1.52 µm.

Discussion

Gall rust disease in falcata, caused by *U. falcatariae*, disperses its teliospores into the air, facilitating widespread transmission in areas with high relative humidity and low wind speed (Rahayu et al. 2010; Rahayu 2018; Wood 2022). The disease has been present in the Philippines since 1989 (Eusebio 1998). Lacandula et al. (2017) reported severe

infections of gall rust disease in higher elevations (400-600 m asl) of falcata plantations, with slight occurrences at lower elevations (below 250 masl). Similar results were observed in studies by Rahayu et al. (2018) in Malaysia, Tulod et al. (2024), and Casilac and Tulod (2024) in Mindanao, Philippines, highlighting the influence of elevation on the severity and incidence of gall rust disease. The study by Palma et al. (2020) also noted similar findings in falcata species under agroforestry systems.

The fungus affects all growth stages of falcata, including stems, branches, leaf petioles, and shoots, producing galls through hypertrophy, hyperplasia, or both as responses to the infection (Rahayu et al. 2009; Rahayu et al. 2010). The current study also observed gall formation on the leaf rachis. Gall rust disease negatively impacts the growth performance and morphological structure of susceptible falcata trees, leading to reduced production and wood quality (Rahmawati et al. 2019; Tulod et al. 2024).

This study further explored how elevation influenced the morphological characteristics of the teliospores. It was found that teliospore dimensions increased significantly with elevation, with the largest dimensions observed at high elevations. These morphological changes may result from the fungus's interactions with its host and environmental factors, suggesting potential evolutionary adaptations. However, the understanding of evolutionary changes and the relationships between these factors remains limited and requires further investigation (Aguilar-Trigueros et al. 2023). The findings on teliospore dimensions may help assess the severity of gall rust disease in falcata plantations, including the survival of teliospores in the field after dissemination. Moreover, significant interactions between elevation, temperature, site factors such as stand density, distance from natural vegetation, and understory vegetation diversity (Tulod et al. 2024), along with high relative humidity and low wind speed, influence disease development (Rahayu et al. 2018). These factors may also affect the fungus's morphological characteristics and warrant further study.

Rust fungi are known for their complex life cycle, particularly in spore dispersal and survival under varying environmental conditions before reaching a suitable host (Helfer 2014). Larger spores have higher sedimentation rates than smaller ones, which travel longer distances but are more exposed to adverse conditions, affecting their survival (Watkinson et al. 2015; Golan and Pringle 2017). Zhao et al. (2022) found that larger spores of *Corynespora cassiicola* exhibited greater virulence under favorable temperature and moisture conditions, resulting in higher spore production. Li et al. (2011) also noted that larger spores demonstrated more virulent characteristics, leading to faster germination. Environmental factors such as high humidity, host uniformity, nutrient availability, and global movements contribute to rust fungi infections and epidemics (Helfer 2014). These factors may uniquely influence the infection dynamics and survival of *U. falcatariae* under field conditions, particularly at higher elevations, warranting further investigation. This highlights the need for a monitoring scheme based on its morphological characteristics across elevations in falcata plantations to develop effective management strategies against the rust fungus.

The study also revealed that the germ pore and dorsal concave diameters of fungal teliospores varied with elevation, with larger dimensions observed at higher elevations. The germ pore and dorsal concave are critical structures used to identify, classify, and characterize obligate parasitic fungi like rust (Yepes and Alves de Carvalho Júnior 2014; Doungsa-Ard et al. 2015; Wood 2019; Ijaz et al. 2022). The germ pore serves as the opening through which the germ tube occurs during fungal spore germination and infection (Gauthier et al. 2014; Singh et al. 2020).

Although the morphological characteristics of the teliospores were similar across different elevations in terms of LM, quantitative measurements of the teliospore dimensions varied. These morpho-features are consistent with previous reports (Doungsa-Ard et al. 2015; Doungsa-Ard et al. 2018; Wood 2019; Wood 2022; Lelana et al. 2022). In contrast, scanning electron microscopy (SEM) revealed varying morphological characteristics of the teliospores from the apical, dorsal, and equatorial views. The major surface structures—apical germ pores, dorsal concave, and longitudinal equatorial striae that is covered with verrucose structures that is particularly denser at high elevations, a feature not typically observed under LM. These results, consistent with other SEM studies (Yepes and Alves de Carvalho Júnior 2014; Chen et al. 2021; Ijaz et al. 2022), provide valuable insights into the classification and identification of the fungus based on microscopic surface features.

The observed variations in the teliospore's quantitative morphological characteristics are crucial for understanding the fungus's dispersal mechanisms, infection, survival, and spread of the disease in falcata trees. Rahayu et al. (2010) reported that the rust fungus can directly penetrate the host epidermis, with visible pustules appearing seven days after inoculation. *U. falcatariae* is classified as a micro-cyclic rust fungus, producing two spore types: basidiospores and teliospores, or pycniospores and teliospores (Doungsa-Ard et al. 2018; Lorrain et al. 2019; Wood 2022). Teliospores have thick walls, enabling dormancy and survival in harsh environmental conditions (Watkinson et al. 2015; Wood 2019).

The fungus, *U. falcatariae,* is characterized as a newly identified species complex of *U. tepperianum*, showing distinct variations in the number of striations on the teliospore. These variations range from 25 to 32 striae, as reported from the Philippines and Timor Leste, compared to the earlier reported range of 30-45 striae (Doungsa-Ard et al. 2015). A study by Lelana et al. (2022) on the teliospores of gall rust in Indonesia revealed a broader range of 25-38 striae. Similarly, the current study also identified an extended range of 25-40 striae in the fungal teliospores, observed across different elevations under SEM. Notably, previous observations were made using LM, highlighting potential differences in spore measurement methodologies.

Despite the variation in terms of the range in the number of striae in the fungal teliospores, the study observed a minimum range of 25-28 striae across different elevations, sharing the same result observed by Lelana et al. (2022),

but was varied on the maximum range of 34-38, which are collected from different provinces in Indonesia. On the other hand, while the current study revealed a higher range from 35-40 striae. Furthermore, the study of Doungsa-Ard et al. (2015) reported a minimum of 25 striae and a maximum of 32, which was lower than the current study, and the latter report for *U. falcatariae* in falcata and *U. tepperianum* group varied at a minimum range of 30-35 and a maximum of 38-45 striae.

In conclusion, this study demonstrates that teliospore length and width of the gall rust fungus in falcata plantations increase with elevation, with significant size increases at moderate to high elevation levels. The germ pore and dorsal concave structures vary across elevations, with the largest dimensions observed at high elevations. Additionally, the number of striations in the fungal teliospores falls within a range of 25-28 striae, similar to previous reports, but the maximum range varies. LM and SEM provide valuable quantitative data for the taxonomy and morphological classification of *U. falcatariae*. High-resolution microphotographs and detailed descriptions of teliospores across different elevations enhance the understanding and identification of the fungus.

These findings highlight the importance of elevation in shaping the morphological traits of the gall rust fungus, which is crucial for developing effective disease management strategies at higher elevations. Further studies, including in vitro and in vivo assessments and correlation studies, are recommended to further characterize the gall rust fungus in conjunction with molecular approaches, ensuring a comprehensive understanding of its characteristics and contributing to the development of control measures for this pathogenic fungus.

ACKNOWLEDGEMENTS

This paper is from the thesis of the principal author. The author gratefully acknowledges DOST-PCAARRD through the Graduate Research and Education Assistantship for Technology (GREAT) program and Ecosystems Research and Development Bureau -Forest and Wetland Research Development and Extension Center (ERDB-FWRDEC). Additionally, DENR Caraga- Community Environment and Natural Resources Office - Bayugan City and Simbalan Mabongahon Workers Association Incorporated (SMAWA) are acknowledged for the site information and assistance during sample collection. The author also would like to thank For. Conrado B. Marquez, For. Joan S. Gilbero, For. Mitch T. Bengil, Jhun Mark Palacio, For. Janrelle Guzon, and Jesie Preglo for the substantial support.

REFERENCES

Aguilar-Trigueros CA, Krah FS, Cornwell WK, Zanne AE, Abrego N, Anderson IC, Powell JR. 2023. Symbiotic status alters fungal eco-evolutionary offspring trajectories. Ecol Lett 26 (9): 1523-1534. DOI: 10.1111/ele.14271.

Alipon MA, Bondad EO, Gilbero DM, Jimenez JP, Domingo EP, Marasigan OS. 2021. Anatomical properties and utilization of 3-, 5-, and 7-yr-old falcata (*Falcataria moluccana* (Miq.)) Barneby & JW Grimes] from Caraga Region, Mindanao Philippines. Philippine J Sci 150 (5): 1307-1319. DOI: 10.56899/150.05.38.

Casilac Jr, C, Tulod AM. 2024. Biophysical factors influencing the height and diameter structures of falcata (*Falcataria falcata* (L.) Greuter & R. Rankin) in Agusan del Norte, Philippines. J Biodivers Environ Sci 24 (3): 202-211. DOI: 10.2139/ssrn.4853852.

Chen CC, Liu HY, Chen CW, Schneider H, Hyvönen J. 2021. On the spore ornamentation of the microsoroid ferns (Microsoroideae, Polypodiaceae). J Plant Res 134: 55-76. DOI: 10.1007/s10265-020-01238-4.

Chowdhury RM, Sternhagen J, Xin Y, Lou B, Li X. Li C. 2022. Evolution of pathogenicity in obligate fungal pathogens and allied genera. PeerJ 10: e13794. DOI: 10.7717/peer j.13794 .

Doloriel NS. 2017. Marketing practices of falcata growers in Tagbina, Surigao Del Sur, Philippines. Intl J Contemp Appl Res 4 (6): 54-61.

Doungsa-ard C, McTaggart AR, Geering AD, Dalisay TU, Ray J, Shivas RG. 2015. *Uromycladium falcatarium* sp. nov. the cause of gall rust on *Paraserianthes falcataria* in south-east Asia. Aust Plant Pathol 44: 25-30. DOI: 10.1007/s13313-014-0301-z.

Doungsa-Ard C, McTaggart AR, Geering ADW, Shivas RG. 2018. Diversity of gall-forming rusts (*Uromycladium*, Pucciniales) on *Acacia* in Australia. Persoonia 40: 221-238. DOI: 10.3767/persoonia.2018.40.09.

Eusebio MA. 1998. Pathology in forestry. Ecosystems Research and Development Bureau, Department of Environment and Natural Resources, College Laguna.

FMB-DENR [Forest Management Bureau of the Department of Environment and Natural Resources]. 2021. Philippine Forestry Statistics. Forest Management Bureau-Department of Environment and Natural Resources (FMB-DENR), Philippines.

Gauthier NW, Maruthachalam K, Subbarao KV, Brown M, Xiao Y, Robertson CL, Schneider RW. 2014. Mycoparasitism of *Phakopsora pachyrhizi*, the soybean rust pathogen, by *Simplicillium lanosoniveum.* Biol Control 76: 87-94. DOI: 10.1016/j.biocontrol.2014.05.008.

Golan JJ, Pringle A. 2017. Long-distance dispersal of fungi. Microbiol Spectr 5 (4): FUNK-0047-2016. DOI: 10.1128/microbiolspec.FUNK-0047-2016.

Han S, Sebastin R, Lee KJ, Wang X, Shin MJ, Kim SH, Chung JW. 2021. Interspecific variation of seed morphological and micro-morphological traits in the genus *Vicia* (Fabaceae). Microsc Res Tech 84 (2): 337-357. DOI: 10.1002/jemt.23592.

Helfer S. 2014. Rust fungi and global change. New Phytol 201 (3): 770-780. DOI: 10.1111/nph.12570.

IBM Corp. 2016. IBM SPSS Statistics for Windows, Version 24.0. IBM Corp, Armonk, NY.

Ijaz M, Afza R, Zafar M, Hamayun M, Khan SM, Ahmad Z, Yahya M. 2022. Taxonomic investigation of selected rust fungi using scanning electron microscopy from Khyber Pakhtunkhwa, Pakistan. Microsc Res Tech 85 (2): 755-766. DOI: 10.1002/jemt.23947.

Khan AS, Ahmad M, Zafar M, Athar M, Ozdemir FA, Gilani SAA, Khan SU. 2020. Morphological characterization of Hypnaceae (Bryopsida, Hypnales): Investigating four genera from Western Himalayas by using LM and SEM techniques. Microsc Res Tech 83 (6): 676-690. DOI: 10.1002/jemt.23458.

Krisnawati H, Varis E, Kallio MH, Kanninen M. 2011. *Paraserianthes falcataria* (L.) Nielsen: Ecology, Silviculture, and Productivity. CIFOR, Bogor, Indonesia.

Lacandula RL, Rojo MJ, Puno GR, Casas JV. 2017. Geospatial analysis on the influence of biophysical factors on the gall rust prevalence in falcata (*Paraserianthes falcataria* L. Nielsen) plantation in Gingoog City, Philippines. J Biodivers Environ Sci 11 (4): 18-24.

Lelana NE, Wiyono S, Giyanto Siregar IZ, Anggraeni I. 2022. Phylogenetic and morphological characteristics of *Uromycladium falcatariae*, the fungal pathogen that causes gall rust epidemics of *Falcataria moluccana* in Indonesia. J Phytopathol 170 (9): 598-604. DOI: 10.1111/jph.13123.

Li CH, Cervantes M, Springer DJ, Boekhout T, Ruiz-Vazquez RM, Torres-Martinez SR, Heitmsn J, Lee SC. 2011. Sporangiospore size dimorphism is linked to virulence of *Mucor circinelloides*. PLoS Pathog 7 (6): e1002086. DOI: 10.1371/journal.ppat.1002086.

Lorrain C, Gonçalves dos Santos KC, Germain H, Hecker A, Duplessis S. 2019. Advances in understanding obligate biotrophy in rust fungi. New Phytol 222 (3): 1190-1206. DOI: 10.1111/nph.15641.

Marasigan OS, Razal RA, Carandang WM, Alipon MA. 2022. Physical and mechanical properties of stems and branches of falcata (*Falcataria moluccana* (Miq.) Barneby & JW Grimes) grown in Caraga, Philippines. Philipp J Sci 151: 575-586. DOI: 10.56899/151.02.03.

Palma RA, Tiongco LE, Canencia OP, Boniao RD, Florida EJ, Dagonio JY. 2020. Gall rust disease incidence of falcata (*Paraserianthes falcataria* (L.) Nielsen) in falcata-based agroforestry systems in Misamis Oriental, Philippines. IOP Conf Ser: Earth Environ Sci 449 (1): 012035. DOI: 10.1088/1755-1315/449/1/012035.

Rahayu S, Lee SS, Shukor NAA. 2010. *Uromycladium tepperianum*, the gall rust fungus from *Falcataria moluccana* in Malaysia and Indonesia. Mycoscience 51 (2): 149-153. DOI: 10.1007/S10267-009-0022-2.

Rahayu S, See LS, Shukor, NAA, Saleh G. 2018. Environmental factors related to gall rust disease development on *Falcataria moluccana* (Miq.) Barneby & Jw Grimes at Brumas Estate, Tawau, Sabah, Malaysia. Appl Ecol Environ Res 16 (6): 7485-7499. DOI: 10.15666/aeer/1606_74857499.

Rahayu S, Shukor NAA, Lee SS, Shaleh G. 2009. Responses of *Falcataria moluccana* seedlings of different seed sources to inoculation with *Uromycladium tepperianum*. Silvae Genetica 58 (1-6): 62-68. DOI: 10.1515/sg-2009-0008.

Rahayu S, Triyogo A, Widyastuti SM, Ardianyah F. 2021. Pests and diseases on *Falcataria moluccana* trees in agroforestry systems with pineapple in East Java, Indonesia. Biodiversitas 22 (5): 2779-2788. DOI: 10.13057/biodiv/d220541.

Rahmawati D, Khumaida N, Siregar UJ. 2019. Morphological and phytochemical characterization of susceptible and resistant sengon (*Falcataria moluccana*) tree to gall rust disease. Biodiversitas 20 (3): 907-913. DOI: 10.13057/biodiv/d200340.

Rojas-Sandoval J. 2023. *Falcataria moluccana* (batai wood). CABI Compendium 38847. DOI: 10.1079/cabicompendium.38847.

Santos Martin F, Lusiana B, Van Noordwijk M. 2010. Tree growth prediction in relation to simple set of site quality indicators for six native tree species in the Philippines. Intl J For Res 2010: 507392. DOI: 10.1155/2010/507392.

Singh Vaibhav K, Aggarwal R, Saharan MS, Jha S. 2020. Pathophenotyping and genome guided characterization of rust fungi infecting wheat and other cereals - A training manual. ICAR-Indian Agricultural Research Institute, New Delhi.

Tulod AM, Casas JV, Rojo MJA, Marin RA, Talisay AM, Bruno EN, Branzuela NE, Solis EB, Bayang SS, Gilbero JS, Loquez MO, Praca EM, Gilbero DM. 2024. Strategies for falcata (*Falcataria falcata* (L.) Greuter and R.Rankin) farmers to mitigate gall rust severity across elevations. Davao Res J 15 (3): 45-50. DOI: 10.59120/drj.v15i3.241.

Watkinson SC, Boddy L, Money N. 2015. The Fungi. Academic Press, New York.

Wood AR. 2019. *Uromycladium* spp. that cause gall rusts (*Acacia* gall rusts). CABI Compendium. DOI: 10.1079/cabicompendium.55738.

Wood AR. 2022. *Uromycladium spp.* that cause gall rusts (*Acacia* gall rusts), PlantwisePlus Knowledge Bank. DOI: 10.1079/pwkb.species.55738.

Yepes MS, Alves de Carvalho Júnior A. 2014. Two new rust species on Fabaceae from Brazil. Mycotaxon 128 (1): 17-23. DOI: 10.5248/128.17.

Zhao Q, Shi Y, Wang Y, Xie X, Li L, Fan T, Li B. 2022. Temperature and humidity regulate sporulation of *Corynespora cassiicola* that is associated with pathogenicity in cucumber (*Cucumis sativus* L.). Biology 11 (11): 1675. DOI: 10.3390/biology11111675.